A Non-invasive Method for Measuring Blood Flow Rate in Superficial Veins from a Single Thermal Image

Ali Mahmoud, Ahmed EL-Barkouky, Heba Farag, James Graham, Aly Farag
Electrical and Computer Engineering Department, University Of Louisville
{ali.mahmoud, ahmed.elbarkouky, heahme01, james.graham, aly.farag}@louisville.edu

Abstract

In this paper, we propose a thermal image based measurement technique for the volumetric flow rate of a liquid inside a thin tube. Our technique makes use of the convection heat transfer dependency between the flow rate and the temperature of the flowing liquid along the tube. The proposed method can be applied to diagnose superficial venous disease non-invasively by measuring the volumetric blood flow rate from a FLIR LWIR single thermal image.

1. Introduction

Measuring the blood flow rate plays an important role in many medical applications among which is vascular disease diagnosis. Vascular disease is a disorder that occurs in the blood vessels which can lead to improper human blood circulation. Among vascular diseases are arterial disease that affects arteries which carry oxygen-rich blood from the heart to the body organs, and venous disease that affects veins which carry blood back from the organs to the heart to be purified. Regarding the veins, they can be categorized into deep veins which are located deep away from the human skin surface, and superficial veins which are located near the skin surface. Of concern in this paper, we focus on superficial venous disease which can be practically diagnosed using a thermal image.

Superficial veins can be affected by thrombophlebitis [1] that is the development of a blood clot in the vein lowering the blood flow rate in it. And since superficial veins are responsible for transferring heat between the blood and the surrounding environment through the skin, a low blood flow rate in these veins can lead to an improper heat transfer process and improper temperature of the skin in the region of the affected vein. For instance, if it is supposed for warm blood in a certain superficial vein to give out a certain amount of heat, it can lose more amount due to low flow as the blood will flow for a longer time through its surrounding cooler tissues leading to more heat loss which rises the temperature of these tissues. This is clear through thermal imaging as the temperature of the skin in an abnormal region appears higher than that in a normal region as illustrated by Bagavathiappan et al. [1]. Other related works are presented in [2, 3, 4]. In [2], Ratovoson et al. used thermal imaging to study the effect of strong thermal variations on thermomechanical behavior of the skin which can be applied for body burns. They extended their work in [4] by presenting a numerical model to simulate the average blood velocity in veins under thermal stress in which metabolism and blood perfusion effects are negligible. Boué et al. [3] presented a thermal model for the forearm and estimated the blood flow by using a heating source to stimulate a skin.

In this paper, we interpret the work of [1] in a quantitative manner in which a single thermal image of superficial veins can not only detect that abnormality but also can measure the blood flow rate through veins, pressure drop along the veins and the amount of heat lost due to the shear stress exerted by the viscosity of the blood. Throughout this work, we will assume blood to be a Newtonian [5] incompressible fluid whose flow is laminar. Blood vessels will be modeled as cylindrical tubes in which the flowing blood loses heat by convection to the surroundings. Moreover, time-average velocity is used to deal with pulsatile flow as steady state flow [6]. Our experiments will contain two parts: 1) validating our concept by building a setup that simulates superficial veins, and 2) vivo measurement validation for a human subject.

A brief discussion of laminar flow will be given in Sec. 2 focusing on heat transfer in a cylindrical tube by convection and how the temperature of the flowing fluid is related to the flow rate. Sec. 3 discusses heat transfer for superficial veins. Thermal imaging concepts will be described in Sec. 4. Finally, Sec. 5 describes our experimental setup and results.

2. Laminar flow inside a tube

In Laminar flow, the fluid streamlines are parallel [7] and orderly slide over each other while in turbulent flow, irregularity occurs to the flow pattern as adjacent layers mix with each other. In order to determine the type of the flow inside a cylindrical tube, Reynold's number R_e [8] should be calculated:

$$R_e = \frac{\rho u_{avg} D}{\mu}, \quad (1)$$

978-0-7695-4990-3/13 $26.00 © 2013 IEEE
DOI 10.1109/CVPRW.2013.60

IEEE computer society

where μ and ρ are the fluid dynamic viscosity and density respectively, and u_{avg} is the average fluid velocity inside the tube whose inner diameter is D.

If R_e <2000, the flow is laminar and if R_e >4000 the flow is turbulent. For values between 2000 and 4000, the flow can be either laminar or turbulent (critical flow [8]). In this paper, we will restrict our work to the case of laminar flow i.e. we will deal only with flow with R_e <2000. This is why we will deal with thin tubes as lowering D means lowering R_e.

2.1. Flow rate using convection heat transfer

Forced convection [9] refers to the presence of heat transfer along with a fluid flow inside a solid (e.g. a tube) under the effect of an external influence (e.g. a pump) when the fluid and the solid are at different temperatures. For a tube, the heat transfer occurs from the fluid to the tube wall if the temperature of the fluid is higher than that of the tube wall and occurs from the tube wall to the fluid if the temperature of the tube wall is higher. We will consider the later case in deriving the equations in this section. However, the obtained equations will be also valid for the other case. Although a fluid can be either a liquid or a gas, this paper deals with liquids only.

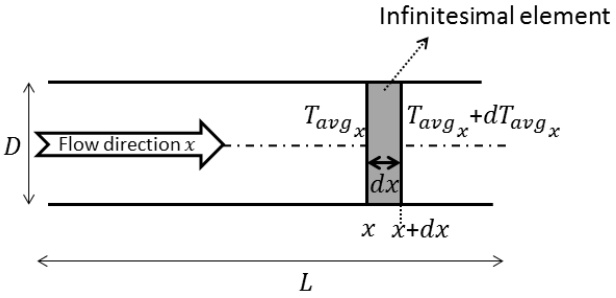

Figure 1: Cylindrical tube in which fluid average temperature changes by dT_{avg_x} along an infinitesimal element of length dx.

The convection heat transfer is composed of two mechanisms [9]: heat transfer due to diffusion and heat transfer by the bulk motion of the liquid taking into account that the contribution in heat transfer due to bulk motion of the liquid is dominant over diffusion. Consider the cylindrical tube portion shown in Fig. 1 in which D, and L are the inner diameter, and length respectively. For an infinitesimal cylindrical element of length dx, the rate of convection heat transfer per unit area of the surface of that element is known as the convection heat flux and is given by Newton's law of cooling [9] as:

$$q_{conv}'' = h_c(T_w - T_{avg_x}), \tag{2}$$

where h_c is the local convection heat transfer coefficient and T_{avg_x} is the liquid temperature averaged over the tube inner radius at an arbitrary point x. Applying the law of conservation of energy, the rates of energy entering and exiting the mentioned infinitesimal volume should be equal. Thus the convection heat transfer rate should equal the sum of the rate of increase in the thermal energy of the liquid and the rate of the work done by the flow through the mentioned infinitesimal volume and hence the rate of convection heat transfer between x and $x + dx$ is given by:

$$dq_{conv} = \dot{m}c_p dT_{avg_x}, \tag{3}$$

where c_p is the liquid specific heat at constant pressure and $\dot{m}$ is the mass flow rate which is related to the volumetric flow rate $\dot{V}$ by:

$$\dot{m} = \rho\dot{V}\ . \tag{4}$$

And from the definition mentioned above of the convection heat flux and having the surface area of the infinitesimal element $\pi D dx$, dq_{conv} can be written also as

$$dq_{conv} = q_{conv}''\pi D dx. \tag{5}$$

Equating Eq. (3) and Eq. (5), gives:

$$\frac{dT_{avg_x}}{dx} = \frac{q_{conv}''\pi D}{\dot{m}c_p}. \tag{6}$$

Integrating Eq. (6) from 0 to x while assuming constant heat flux at the tube wall gives T_{avg_x} varying linearly with x as:

$$T_{avg_x} = T_{avg_0} + \frac{q_{conv}''\pi D}{\dot{m}c_p}x, \tag{7}$$

where T_{avg_0} is the average temperature of the liquid at the entrance of the tube portion. And for laminar flow [9], $h_c = 4.36\frac{k}{D}$ assuming fully developed thermal conditions, where k is the thermal conductivity of the liquid. Thus substituting for the values of q_{conv}'' from Eq. (2) and $\dot{m}$ from Eq. (4), Eq. (7) is reduced to:

$$T_{avg_x} = T_{avg_0} + \frac{4.36k(T_w - T_{avg_x})\pi}{\rho\dot{V}c_p}x. \tag{8}$$

Substituting for x by L in the previous equation and arranging it gives the liquid volumetric flow rate $\dot{V}$ as:

$$\dot{V} = \frac{4.36k\pi L(T_w - T_{avg_L})}{\rho c_p(T_{avg_L} - T_{avg_0})}. \tag{9}$$

2.2. Pressure drop and power loss due to friction

Consider a portion of length L of the cylindrical tube as shown in Fig. 2. Assuming the motion of the liquid inside the tube to be frictionless i.e. neglecting the viscosity

effect, Bernoulli's principle [10] implies that the sum of kinetic energy and potential energy along the stream tube remains constant, and hence, the sum of the static pressure, dynamic pressure, and gravitational pressure remains constant:

$$p + \frac{1}{2}\rho u^2 + \rho g z = constant, \quad (10)$$

where p is the liquid static pressure, $\frac{1}{2}\rho u^2$ is the dynamic pressure, and $\rho g z$ is the gravitational pressure with u, g and z being the liquid velocity, gravitational acceleration and height with respect to a given reference level respectively.

Considering point 1 and point 2 at the beginning and end of the tube portion respectively, Eq. (10) becomes:

$$p_1 + \frac{1}{2}\rho u_1^2 + \rho g z_1 = p_2 + \frac{1}{2}\rho u_2^2 + \rho g z_2 \quad (11)$$

Practically, the effect of liquid viscosity should be taken into account, as liquid viscosity is a measure of its resistance to shape change brought by shear stresses between liquid layers and between liquid and tube walls. The shear stress between the liquid and the tube walls causes friction that is dissipated in the form of heat. That shear stress acts along the inner surface of the tube portion whose surface area is $\pi D L$ and exerts a force in a direction opposing the flow. In order to overcome that force, a pressure drop Δp occurs inside the tube portion [10, 11] which modifies Eq. (11) to:

$$p_1 + \frac{1}{2}\rho u_1^2 + \rho g z_1 = p_2 + \frac{1}{2}\rho u_2^2 + \rho g z_2 + \Delta p. \quad (12)$$

The pressure drop Δp can be interpreted into a force acting on the tube inner cross sectional area $\frac{\pi D^2}{4}$. This force is equal in magnitude to the force exerted by the shear stress [7]. The velocity profile across the tube for laminar flow is parabolic with maximum value at the centerline of the tube and zero values at the tube walls [11] given by:

$$u = -\frac{D^2}{16\mu}\frac{dp}{dx}\left(1 - \left(\frac{2r}{D}\right)^2\right), \quad (13)$$

where dp is the pressure drop occurring along an infinitesimal cylindrical element of length dx and height r, and coaxial with the centerline of the tube with the positive x direction being the direction of the flow as shown in Fig. 2.

Since the velocity is not uniform across the tube, integration should be used when calculating the volumetric flow rate $\dot{V}$. Consider dealing with a thin shell of thickness dr at a distance r form the tube centerline. The shell cross sectional area $dA = 2\pi r dr$ and the volumetric flow rate through that shell $d\dot{V}$ is given by:

$$d\dot{V} = u\, dA. \quad (14)$$

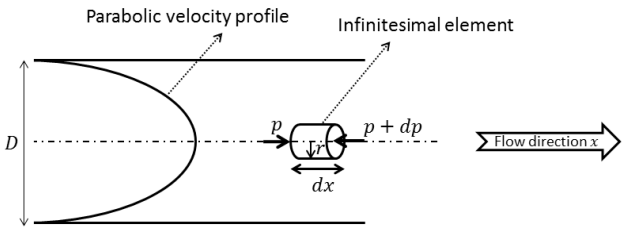

Figure 2: Parabolic velocity profile for a cylindrical tube with laminar flow

Substituting Eq. (13) into Eq. (14) and integrating r across the tube from 0 to $\frac{D}{2}$ gives:

$$\dot{V} = -\frac{\pi}{128\mu}\frac{dp}{dx}D^4\,. \quad (15)$$

Assuming uniform flow during the tube portion under consideration, $\frac{dp}{dx}$ is a constant [11] and thus can be replaced by $-\frac{\Delta p}{L}$ and hence Eq. 15 is simplified to:

$$\Delta p = \frac{128\mu L}{\pi D^4}\dot{V}. \quad (16)$$

From the first law of thermodynamics (conservation of energy) [7], the power loss P_{loss} due to a pressure drop Δp is given by:

$$P_{loss} = \dot{V}\Delta p, \quad (17)$$

substituting for Δp from Eq. (16) gives:

$$P_{loss} = \frac{128\mu L}{\pi D^4}\dot{V}^2. \quad (18)$$

From Eq. (16) and Eq. (18), it is clear that succeeding to measure the volumetric flow rate $\dot{V}$ leads directly to the knowledge of Δp and P_{loss} .

The liquid properties as the viscosity, density, thermal conductivity, and specific heat capacity are temperature dependent but can be practically found at the reference temperature [9] and then assumed to be constant along the tube. The reference temperature is found by averaging the mean temperatures of the liquid at the inlet and the outlet of the tube.

3. Blood vessel convective heat transfer

In this paper, we focus on superficial veins which can be practically seen in a thermal image. While blood flows in the veins, heat is exchanged between the blood and the surrounding tissues [12]. Penne [13] in 1948 showed that blood flow acts as a warming agent for the superficial veins while studying the forearm. He assumed that there are two main heat sources in the tissues, which are heat transfer from blood to the tissues and heat generated in the tissue by metabolism. The later occurs at a low rate near the surface of the forearm. He stated that the rate of heat transfer from the blood to the tissue at a certain location is

proportional to the difference between the blood temperature and the tissue temperature.

The tissues surrounding blood veins can be modeled as solid [2]. Thus assuming a superficial blood vein to be a very thin cylindrical shell surrounded by these solid tissues, and assuming blood to be a Newtonian [5] incompressible laminarly flowing fluid for which time-average velocity is used to deal with pulsatile flow -due to heart beating- as steady state flow [6], we can formulate the heat transfer between the flowing blood and the surrounding tissues as a case of forced convection heat transfer in a cylindrical [14] tube under laminar flow. Thus, the equations presented in the previous section can be applied directly to our case. Analyzing Eq. (9), it is clear that the difference between the inlet and outlet blood temperatures of a certain vein is inversely proportional to volumetric blood flow rate. This quantitatively clarifies the reason for the improper heat transfer and improper temperature of the skin in the region of a superficial vein that is affected by thrombophlebitis [1], and hence increases the drop in the temperature of the blood exiting the vein with respective to its temperature at the inlet. In other words, superficial veins are responsible for transferring heat between the blood and the surrounding environment through the skin, so if it is supposed for warm blood in a certain superficial vein to give out a certain amount of heat, it can lose more amount due to low flow as the blood will flow for a longer time through its surrounding cooler tissues leading to more heat loss which rises the temperature of these tissues and decreases the temperature of the blood.

In this paper, we will validate this concept by observing the effect of varying the flow rate of a liquid flowing in a cylindrical tube on the difference in the temperatures of the liquid entering and exiting that tube. These temperatures will be fed into Eq. (9) to get an estimate of the volumetric flow rate and compare it with ground truth. The estimated volumetric flow rate can then be fed into Eq. (16) and Eq. (18) to get an estimate for the pressure drop and power lost by the viscosity respectively. Another part of our experiments is to image the superficial veins in the forearm of a living human subject and see the effect of lowering the blood flow rate on the difference in the temperatures of the blood entering and exiting a superficial vein. The temperature in our experiments will be estimated using thermal imaging which is briefly discussed the next section.

4. Thermal imaging basics

The concept of thermal imaging arose from studying the phenomenon of Blackbody radiation [15]. A blackbody at a temperature T above 0 K continuously absorbs and then diffusely reemits photons (light quanta) of all possible wavelengths λ (λ ranges from 0 to ∞). It was found that the number of photons emitted per unit wavelength at a certain wavelength is dependent on T. This is clear in Planck's law which gives the radiation spectral intensity of a blackbody at temperature T as [15]:

$$B_\lambda(T) = \frac{2hc^2}{\lambda^5}\frac{1}{e^{\frac{hc}{KT\lambda}}-1}, \tag{19}$$

where $h = 6.625 \times 10^{-34}$ J s (Planck's constant), $K = 1.37 \times 10^{-23}$ J K^{-1} (Boltzmann's constant) and $C = 3 \times 10^8$ m s^{-1} (light speed). If the peak of Eq. (19) occurs at λ_{max}, the product of λ_{max} and T is a constant given by Wien displacement law [16] as:

$$\lambda_{max}T = 2.897 \times 10^{-3} \text{ m K}. \tag{20}$$

As a result, the dominant emitted wavelength is in the visible light range for an extremely high temperature body (thousands of kelvins). As the body temperature gets lower, the dominant wavelength moves towards the infrared regions (NIR, SWIR, MWIR, LWIR).

Integrating Eq. (19) over a hemisphere for $0 < \lambda < \infty$, gives the power radiated per unit area of the emitting surface at temperature T as (Stefan-Boltzmann law [15]):

$$R(T) = \sigma T^4, \tag{21}$$

where $\sigma = 5.67 \times 10^{-8}$ W m^{-2}K^{-4} is the Stefan-Boltzman constant.

For a non-blackbody, beside the phenomenon of temperature based emission of photons, there is also reflection of photons incident from an external visible light source. Since the emitted photons carry information about the body temperature, succeeding in separating that portion of photons from the reflected portion gives the temperature of the body. Fortunately, at low temperature (few hundreds of kelvins), the dominant wavelength of the emitted photons lies in the infrared region, thus they are band separated from the reflected visible photons. Based on this, thermal infrared cameras can give the temperature of a body. An important surface property related to thermal imaging is the emissivity [17] which indicates how well a real object emits radiation compared to a blackbody at the same temperature and wavelength. Emissivity depends on the wavelength and the direction of emission. Taking into account averaged emissivity ε over all wavelengths and all directions, Eq. (21) is modified to:

$$R(T) = \varepsilon\sigma T^4, \tag{22}$$

where the averaged emissivity ε takes values from 0 to 1. In the above discussion, we were assuming dealing with wavelengths from 0 to ∞. Practically, the used thermal camera wavelength band should be taken into consideration.

5. Experimental results

In our experiments, the blood flow will be estimated using thermal images captured by a FLIR LWIR thermal camera operating in the 7.5-13 μm wavelength range with a resolution of 640×480 pixels. The thermal sensitivity of the camera is 50 mK. The IR lens used with the camera has a 41.3 mm focal lens and a 17 micron pixel detector. The thermal camera is mounted vertically at a distance 1 meter from a horizontal tube (or vein). For this setup, 1 pixel in the thermal image represents 396 μm x 396 μm. This spatial calibration was done by taking a thermal image for a hot rod with known length and at a known distance from the lens.

In the first part of the experiment, we will use two cylindrical tubes to simulate superficial veins. One of them has a throttle that causes the liquid flow to be slower simulating a vein with stenosis while the other one has normal flow representing a healthy vein. The tubes will contain water flowing horizontally using a pump that is controlled by a generator to supply either continuous flow or pulsatile flow. The water temperature at the pump is kept at 37 °C while the container (where the tubes are mounted horizontally) contains ice at 0 °C as shown in Fig. 3.

We measure the temperature at the inlet and the outlet of the tubes which will show a drop due to the convection heat transfer from the hot water in the tubes to the ice in the container. This temperature drop is then used in Eq. (9) -which is repeated here for convenience- to calculate the volumetric flow rate in the two tubes as follows:

$$\dot{V} = \frac{4.36k\pi L(T_w - T_{avg_L})}{\rho c_p (T_{avg_L} - T_{avg_0})}. \quad (23)$$

The following values were used for the constants in the equation: $k = 0.626 \frac{\text{J}}{\text{K m s}}$, $\rho = 994.1 \frac{\text{Kg}}{\text{m}^3}$, $c_p = 4178 \frac{\text{J}}{\text{Kg K}}$ and $L = 0.24$ m. Hence the resulting volumetric flow rate should be in m³/s which is equal to 10^6 mL/s. Fig. 4 shows the temperature profile along the cross sections of the tubes at the inputs and outputs where it is clear that the tube with the throttle reduced flow rate of the water leading to more heat loss. This leads to a temperature drop of 1 °C between the input and the output of the throttled tube compared to a temperature drop of 0.45 °C in the regular tube as shown in Fig. 4. For both cases, the difference between the wall temperature and the average temperature is 4.3 °C, hence the flow can be calculated using Eq. (9) to be 2.1 and 4.7 mL/s in the tubes with and without the throttle respectively. The ground truth for these flow rates were measured to be 1.8 and 5.0 mL/s respectively by dividing the volume of water dispensed in each case by the time of the experiment. The target of this part of our experiment was just to validate the theory behind our approach in a setup where the ground truth can be easily measured. This experiment was repeated several times and similar results were obtained. These results show that the proposed method is reliable for estimating the flow.

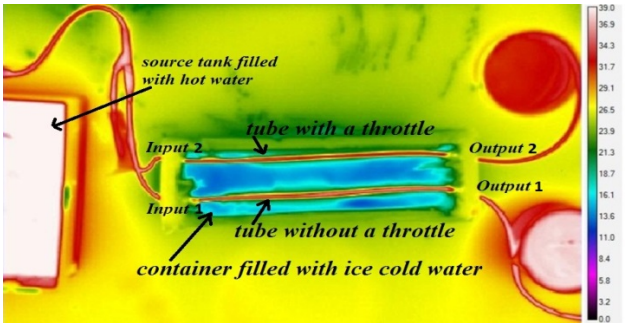

Figure 3: A thermal image showing the first part of our experiment where the upper tube has a throttle while the lower tube is regular.

Feeding the calculated $\dot{V}$ values into Eq (16) and Eq. (18), with a diameter $D = 0.3$ cm and viscosity $\mu = 710 \times 10^{-6} \frac{\text{N.s}}{\text{m}^2}$, leads directly to Δp and P_{loss}.

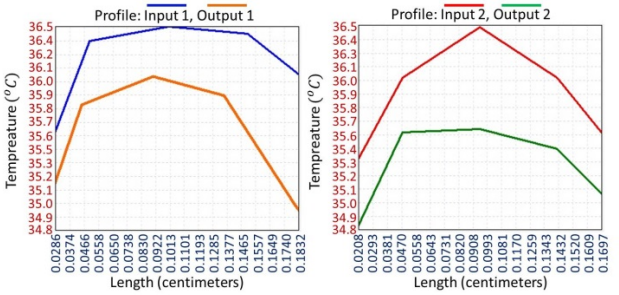

Figure 4: Temperature profiles along the cross sections of the tubes at the inputs and outputs for the tube with a throttle on right and without a throttle on left.

In the second part of our experiment, we apply the same ideas of the first part to a human forearm. We put an ice pack on the forearm so that the blood flowing in the veins will have a temperature drop due to the convection heat transfer. We capture a thermal image for the forearm after putting an ice pack on it as shown in Fig. 5. The temperature of the vein before and after the cold part will be used to calculate the blood flow rate using Eq. (9) as we did in the first part of the experiment.

For validation, we wanted to estimate the blood flow in a subject for a normal vein and compare it with the same subject and the same vein if it has a stenosis. To simulate that, we capture a thermal image for a subject and then we put a thin cuff around the forearm to lower blood flow and capture another thermal image as shown in Fig. 5. By comparing the results we can get a feeling of how the stenosis will reduce the blood flow. The following values were used for the blood at 37 °C: $k = 0.549 \frac{\text{J}}{\text{K m s}}$, $\rho = 1060 \frac{\text{Kg}}{\text{m}^3}$, and $c_p = 3820 \frac{\text{J}}{\text{Kg K}}$. L from the input to the output was measured form the thermal image to be 0.053

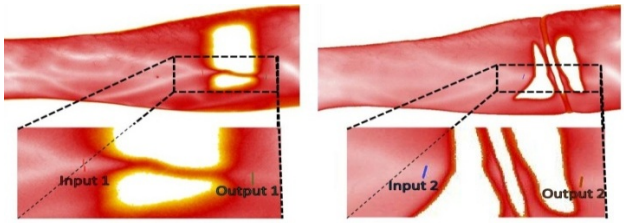

Figure 5: Thermal images showing the right forearm after putting an ice pack over a vein with a cuff around the vein in the right image

m. The input and the output locations should be on the vein before and after the ice pack location respectively. These locations do not have to be in the same physical spots for different images taking into consideration that the distance between them is the length L which is part of Eq. (9). In Fig. 5, we took them such that the distance L is equal in both images but that was not necessary. Fig. 6 shows a temperature drop of 0.7 ℃ between the input and the output of the healthy vein compared to a temperature drop of 0.95 ℃ in the throttled vein. For both cases, the difference between the wall temperature and the average temperature is 0.42 ℃, leading to a blood flow rate of 0.06 and 0.04 mL/s for the regular and stenotic case respectively.

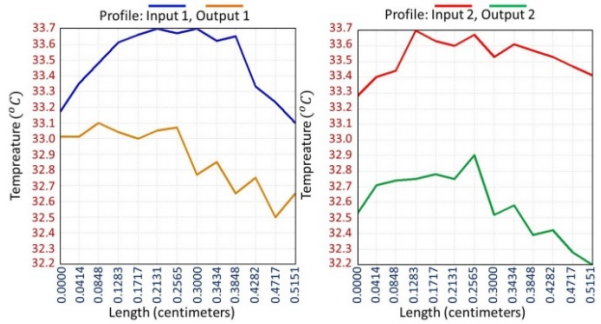

Figure 6: Temperature profiles along the cross sections of a vein at the inputs and outputs for the tube with a cuff on right and without a cuff on left.

6. Conclusion and future work

In this paper, the volumetric flow rate of a liquid inside a thin tube was estimated non-invasively using a single thermal image. Our technique makes use of the difference in the liquid temperatures at the inlet and the outlet of the tube caused by convection heat transfer. That temperature difference was shown analytically and experimentally to be dependent on the volumetric flow rate and thus can be used to give a good estimate for the flow rate. We tested our method with the superficial veins of a human subject forearm. The experiment was done once for the case of regular blood flow and once for stenotic blood flow. We propose to use our technique to non-invasively diagnose superficial venous disease that significantly affects the blood flow in the veins. Although this research was done on normal subjects, we intend to test it in the future with patients having superficial venous disease.

References

[1] S. Bagavathiappan, T. Saravanan, J. Philip, T. Jayakumar, B. Raj, R. Karunanithi,T. Panicker, M. Korath, and K. Jagadeesan. Infrared thermal imaging for detection of peripheral vascular disorders. *J Med Phys*, 34(1):43–47, 2009.

[2] D. Ratovoson, F. Jourdan, and V. Huon. A study of heat distribution in human skin: use of Infrared Thermography. *14th International Conference on Experimental Mechanics*, 2010.

[3] C. Boué, F. Cassagne, C. Massoud, and D. Fournier. Thermal imaging of a vein of the forearm: Analysis and thermal modeling. *Infrared Physics & Technology*, 51(1): 13-20, 2007.

[4] D. Ratovoson, V. Huon, V. Costalat, and F. Jourdan. Combined model of human skin – Heat transfer in the vein and tissue: experimental and numerical study. *Quantitative InfraRed Thermography Journal*, 8(2): 165-186, 2011.

[5] I. Santos, D. Haemmerich, C. Pinheiro, and A. Rocha. Effect of variable heat transfer coefficient on tissue temperature next to large vessel during radiofrequency tumor ablation. *BioMedical Engineering Online*, 11:7-21, 2008

[6] G. Bourantas, E. Skouras, V. Loukopoulos, V. Burganos, and G. Nikiforidis. Two-phase blood flow modeling and mass transport in the human aorta. *10th International Workshop on Biomedical* Engineering, 1-4, 2011.

[7] S Post. *Applied and Computational Fluid Mechanics*. Jones & Bartlett Learning, 2010.

[8] E. Menon. *Liquid Pipeline Hydraulics*. CRC Press, 2004.

[9] F. Incropera, and D. DeWitt. *Introduction To Heat Transfer*. second edition, Wiley, 1990.

[10] C. Rose. *An Introduction to the Environmental Physics of Soil, Water and Watersheds*. Cambridge University Press, Cambridge, UK, 2004.

[11] Z. Warhaft. *An Introduction to Thermal-Fluid Engineering: The Engine and the Atmosphere*. Cambridge University Press, Cambridge, UK, 1998.

[12] D. Haemmerich, A. Wright, D. Mahvi, F. Lee, and J Webster. Hepatic bipolar radiofrequency ablation creates coagulation zones close to blood vessels: A finite element study. *Med Biol Eng Comput*, 41:317-323, 2003.

[13] H. Pennes. Analysis of tissue and arterial blood temperatures in resting human forearm. *Journal of Applied Physiology*, 1:93–122, 1948.

[14] V. Leeuwen, A. Kotte, J. DeBree, J. VanderKoijk, J. Crezee, and J. Lagendijk. Accuracy of geometrical modelling of heat transfer from tissue to blood vessels. *Phys. Med Biol*., 42:1451-1460, 1997.

[15] J. Robert Mahan. *Radiation Heat Transfer, A Statistical Approach*. WILEY, 2002.

[16] Lianxi Ma, Junjun Yang and Jiacai Nie. Two forms of Wien's displacement law. *Lat. Am. J. Phys. Educ*. 3(3):566-568, 2009.

[17] R. Siegel, and J. Howell. *Thermal Radiation Heat Transfer*. Hemisphere Pub. Corp., 1981.